ROLE OF ACOUSTIC CAVITATION IN THE DELIVERY AND MONITORING OF CANCER TREATMENT BY HIGH-INTENSITY FOCUSSED ULTRASOUND

Constantin C. Coussios, Inst. of Biomedical Engineering, Dept. of Engineering Science, University of Oxford, Oxford, UK

Caleb H. Farny, Dept. of Aerospace and Mechanical Engineering, Boston, MA, USA

Gail ter Haar, Institute of Cancer Research, Sutton, UK

Ronald A. Roy, Dept. of Aerospace and Mechanical Engineering, Boston, MA, USA*

Corresponding Author:

Dr Constantin-C. Coussios
Institute of Biomedical Engineering
Department of Engineering Science
University of Oxford
17 Parks Road
Oxford
OX1 3PJ
Tel: +44-1865-274750
Fax: +44-1865-274752
E-mail: constantin.coussios@eng.ox.ac.uk

Running Title:

ROLE OF CAVITATION DURING HIFU

* *Current Address: Department of Engineering Science, 17 Parks Road, Oxford OX1 3PJ, UK*

ABSTRACT

Acoustic cavitation has been shown to play a key role in a wide array of novel therapeutic ultrasound applications. This paper presents a brief discussion of the physics of thermally relevant acoustic cavitation in the context of High-Intensity Focussed Ultrasound (HIFU). Models for how different types of cavitation activity can serve to accelerate tissue heating are presented, and results suggest that the bulk of the enhanced heating effect can be attributed to the absorption of broadband acoustic emissions generated by inertial cavitation. Such emissions can be readily monitored using a passive cavitation detection (PCD) scheme and could provide a means for real-time treatment monitoring. It is also shown that the appearance of hyperechoic regions (or bright-ups) on B-mode ultrasound images constitutes neither a necessary nor a sufficient condition for inertial cavitation activity to have occurred during HIFU exposure. Once instigated at relatively large HIFU excitation amplitudes, bubble activity tends to grow unstable and to migrate towards the source transducer, causing potentially undesirable pre-focal damage. Potential means of controlling inertial cavitation activity using pulsed excitation so as to confine it to the focal region are presented, with the intention of harnessing cavitation-enhanced heating for optimal HIFU treatment delivery. The role of temperature elevation in mitigating bubble-enhanced heating effects is also discussed, along with other bubble-field effects such as multiple scattering and shielding.

Keywords: high intensity focused ultrasound (HIFU), stable cavitation, inertial cavitation, microbubbles, cavitation control, cavitation monitoring, heating, absorption, attenuation, passive cavitation detection (PCD), B-mode ultrasound, hyperechoic, hyperechogenic, pulsed ultrasound, duty cycle, pulse duration.

1. INTRODUCTION

At large rarefaction pressure amplitudes, a propagating ultrasonic wave may place the surrounding tissue under sufficient tension for small cavities, which rapidly fill with gas and vapor, to form. This process is known as acoustically induced cavity nucleation, and the pressure amplitude required to induce such phenomena depends greatly on the physical properties of the medium [1-3]. Once formed, subsequent ultrasonic excitation will cause these bubbles to pulsate volumetrically, a process known as acoustic cavitation [4-9].

Early studies of ultrasonically induced cavitation in tissue were triggered by concerns for the safety of diagnostic ultrasound [10-18]. Experimental studies (performed mostly in small animals) suggested that, at the upper end of the pressure output of diagnostic scanners, tissue damage, which occurred preferentially near gaseous interfaces, could be observed. Concerns about such bioeffects led to the formulation of the Mechanical Index, which gauges the likelihood of cavitation excitation by short-pulse, low-duty-cycle diagnostic ultrasound in the presence of pre-existing gas nuclei [8, 19-21]. Based on this work, operating conditions aimed at minimizing the risk of what was perceived as undesirable bubble activity in a diagnostic context have been proposed for ultrasound scanners [15, 16, 18, 22].

However, the rapid emergence of a wide array of therapeutic ultrasound applications over the last two decades has led to a reevaluation of the desirability of acoustic cavitation in vivo. Ultrasonic waves have been reported to cause potentially beneficial bioeffects, including the sealing of blood vessels (acoustic haemostasis) [23-34], dissolution of blood clots (thrombolysis) [35-46], activation of drugs [47-50], opening of the blood brain barrier [51-61] and the increase of cell membrane and skin permeability to molecules (sonoporation

and sonophoresis) [62-64]. Even though the exact biophysical mechanisms underlying these phenomena remain poorly understood, acoustic cavitation is often acknowledged as their most likely common denominator [65-69].

Many therapeutic applications – particularly those involving rapid tissue heating, acoustic haemostasis, and tissue ablation – employ high intensity beams of focused ultrasound (HIFU) [70-73]. Tissue heating occurs primarily due to viscous absorption of the acoustic energy. Both the attenuation and absorption coefficients in tissue are known to increase as a power law with increasing frequency [74-77], which implies that the choice of clinical HIFU frequencies constitutes a compromise between the desired treatment depth, limited by attenuation, and the maximum achievable rate of heating, determined by absorption [78, 79]. In the context of HIFU ablation in particular, the objective is to induce rapid and irreversible thermal necrosis of malignant tumors, with minimal damage in the intervening path. Any mechanism which might make it possible to increase heat deposition efficiency at the focus whilst minimizing prefocal damage is therefore of great potential interest, and it is in this context that cavitation can play a potentially crucial role.

The peak negative pressures produced by HIFU fields are often sufficiently large to produce cavitation activity which is generally, but not always, initially confined to the focal region of the HIFU field. Recent studies have demonstrated that the presence of small gas bubbles at the ultrasound focus can lead to substantially higher rates of tissue heating, which can be as much as six times the rate of heating in the absence of bubbles [80-84]. This enhanced rate of heating is generally attributed to two basic types of acoustic cavitation activity, described in greater detail in the next section. Stable cavitation is the prolonged linear or nonlinear oscillation of an acoustically driven bubble about its equilibrium radius, where the dynamics

of the cavity motion are dominated by the compressibility of the gas. Inertial (or transient) cavitation describes the unstable expansion of a bubble followed by a rapid, violent collapse dominated by the inertia of the surrounding medium, usually occurring over a single or small number of acoustic cycles [85]. During collapse, inertial cavities will radiate energy into the surrounding tissue in the form of broadband acoustic emissions [86, 87] .

Based on the premise that the local rate of HIFU-induced heating is determined by the local, frequency-dependent absorption coefficient, any mechanism that either increases the high-frequency content of the sound field or extends the length-scales over which viscous absorption can occur will result in enhanced heating. The strong scattering of sound by cavities present within a bubble cloud at the HIFU focus will ‘trap’ acoustic energy within that region, extending the sonic propagation path and leading to greater absorption by viscous dissipation and thermal conduction. In addition, the presence of multiple cavities oscillating in the sound field increases the opportunity for viscous absorption in boundary layers at the bubble surface. Finally, in the presence of inertial cavitation, the frequency dependence of the absorption coefficient dictates that the high-frequency broadband noise emissions produced by the collapsing bubbles will be very readily and locally absorbed.

Based on these three mechanisms, acoustic cavitation has tremendous potential to enhance the heat deposition efficiency during HIFU treatment, as it can lead to preferential heating in the focal region compared to the pre-focal region. Furthermore, if this enhanced heating can be directly correlated with inertial cavitation activity, monitoring the broadband noise emissions produced by collapsing bubbles at frequencies well removed from the main HIFU frequency could make it possible to monitor treatment non-invasively. However, harnessing cavitation activity for optimal HIFU treatment delivery is not without its challenges. The

pressures required to generate cavitation in vivo are generally very high and tissue-specific [1, 88-90]. The use of nucleating agents or particular pre-conditioning excitations may thus be required to instigate and promote cavity formation. The appearance of bubbles in a region of tissue will dramatically alter its acoustic impedance, causing reflection of the incident sound wave and increasing sound intensity in the region proximal to the focal volume. This in turn can cause the migration of the bubble cloud towards the HIFU transducer, resulting in damage to prefocal tissue and shielding of the original focus. These factors can contribute to the formation of HIFU lesions of unpredictable shape [83, 91-95], a feature that is highly undesirable during clinical treatments.

For these reasons, the cavitation nucleation and activity in tissue must be understood, monitored and controlled in order to enhance the delivery and monitoring of HIFU treatment. This paper presents a brief overview of the underlying physics of cavitation, the various mechanisms by which cavitation can enhance heating, some representative experimental results demonstrating the accelerated heating effect, and possible techniques for monitoring thermally relevant cavitation activity in real time.

2. PHYSICS OF THERMALLY RELEVANT CAVITATION

Linear and Non-Linear Bubble Behavior

A bubble exposed to a low amplitude sound field will exhibit small radial oscillations that are symmetric about its equilibrium radius. In this linear regime, its behaviour is analogous to that of a mass-spring-damper system, where the spring represents the compressibility of the gas, the mass the inertia of the surrounding liquid, and the damper any viscous, thermal or radiation losses [96, 97]. For bubbles of equilibrium diameter smaller than 10 microns, the

surface tension at the liquid-gas interface will also contribute significantly to the stiffness of the system [85]. As for any second-order linear system, the acoustic bubble will resonate for a particular excitation frequency, known as the resonance frequency f_0 and given by [97, 98]

$$f_0 = \frac{1}{2\pi}\sqrt{\frac{3\gamma P_0}{\rho R_o^{\,2}} + \frac{4\sigma}{\rho R_o^{\,3}}}\,, \tag{1}$$

where P_0 is the ambient pressure, ρ the density of the liquid, σ the surface tension at the liquid-gas interface, R_0 the equilibrium radius in the absence of sound and γ the polytropic exponent for the gas (an adiabatic process is frequently assumed). Conversely, the equilibrium size R_0 of the bubble that will resonate at a particular excitation frequency f_0 is known as the resonance size. Note that for air bubbles in water possessing radii greater than approximately 5 μm, one can ignore the surface tension term, in which case the resonance frequency and equilibrium radius are inversely proportional to each other. For such a bubble undergoing adiabatic pulsations ($\gamma = 1.4$) at atmospheric pressure, this proportionality constant is approximately 3.26 Hz-m.

In the context of the high ultrasound amplitudes encountered in HIFU, the oscillations performed by the bubble can no longer be deemed small and are generally not symmetric about its equilibrium radius. These large pulsations cause the bubble to respond non-linearly, in a manner that is ultimately determined by the initial bubble size, the spectral content of the incident sound field, the proximity of physical boundaries or other neighboring bubbles, the viscoelastic and interfacial properties of the surrounding medium, the ambient temperature, and the propensity for gas diffusion across the bubble wall. The effect that this large array of parameters has on single and multiple bubble behaviour has been explored in detail elsewhere [85, 97, 99-102] and will not be repeated here.

In order to investigate the salient features of HIFU-driven cavitation behavior, we assume here a single bubble of known equilibrium radius R_o pulsating radially in a Newtonian viscous liquid under the effect of a single-frequency acoustic plane wave of amplitude P_a, in the absence of gas transfer across the bubble wall and well away from physical boundaries. The changes in radius R of a bubble driven in this manner can be described by a force balance equation across the bubble wall, where internal pressures arise from gas compression and vapor pressure, and external pressures arise from surface tension, viscous stress, static fluid pressure and dynamic acoustic pressure fluctuations [103, 104]:

$$\left(1-\frac{\dot{R}}{c}\right)R\ddot{R}+\frac{3}{2}\dot{R}^2\left(1-\frac{\dot{R}}{3c}\right)=\left(1+\frac{\dot{R}}{c}\right)\frac{P\left(\dot{R},R,t\right)}{\rho}+\frac{R}{\rho c}\frac{\partial P\left(\dot{R},R,t\right)}{\partial t} \quad \text{, where}$$

$$P\left(\dot{R},R,t\right)=\left[\left(P_o-P_v-\frac{2\sigma}{R}\right)\left(\frac{R_o}{R}\right)^{3\kappa}+P_v\right]-P_o-\frac{2\sigma}{R}-\frac{4\mu\dot{R}}{R}-P_a\sin\omega t \quad . \tag{2}$$

P_o, σ, P_v, μ, c, and ρ are respectively the ambient pressure, surface tension, vapor pressure, viscosity, sound speed, and density of the surrounding medium. It should be noted that Equation 2 reduces to the aforementioned classic second-order system in the limit of small oscillations and negligible surface tension, *i.e.* for acoustic pressures less than about 0.01 MPa and equilibrium radii greater than 5-10 μm.

Equation 2 is highly nonlinear and suggests a range of possible bubble behaviours that are rich in complexity, yet can be broadly classified into two categories: *stable and inertial cavitation*. Stable cavitation is characterized by essentially repetitive radial oscillations about an equilibrium radius that may or may not change over time due to gradual dissolution, or to growth by a process known as rectified diffusion [99, 105, 106]. When driven at HIFU-relevant amplitudes, a stable response is only likely to be exhibited by larger gas-filled bubbles whose radial excursions are arrested by the inertial mass of the surrounding medium.

Such cavities will generally be on the order of the resonance size or larger. In an aqueous medium driven at 1 MHz and a pressure amplitude of 1 MPa, only those bubbles with radii larger than about 3-5 μm will respond stably. As the HIFU pressure amplitude is raised, this lower size limit also increases.

Probably the most important facet of stable cavitation is the formation of small-scale fluid flows known as cavitation microstreaming [107-110], an effect that is greatly enhanced by the excitation of surface waves on the bubble. These flows occur over scales comparable with the bubble dimensions, and are considered to be one of the key ways by which cavitation can lyse cells, clean surfaces, and promote convective drug delivery [66, 111-113]. Stable cavitation can also promote heat generation due to viscous losses in the boundary layer on the surface of the pulsating bubble. In short, stable cavitation provides a means of converting acoustical energy into mechanical (streaming) and thermal (heating) energy over length scales that are comparable to the bubble size but generally much smaller than an acoustic wavelength.

If a stable gas-filled cavity is driven at sufficiently large pressure amplitudes, the rarefaction portion of the acoustic pressure cycle causes it to grow to a size for which the internal pressure drops to the vapor pressure. The progression from gas-filled microbubble to a growing vapor-filled cavity occurs much more readily if the equilibrium size of the bubble is small at the outset, or if the peak negative pressure is extremely large. During the ensuing compressive phase, the growth is arrested and the vapor-filled bubble proceeds to collapse unstably. By the time the gas pressure builds up to the point where it is dynamically significant, the bubble wall velocity approaches supersonic speeds and the collapse continues, driven by the inertia of the inrushing liquid (hence the name *inertial cavitation*). If this

phenomenon occurs far from any boundaries (or other bubbles), the gas is profoundly compressed, resulting in intense heating and pressure. Chemical reactions ensue and light is generated from the radiative re-combination of chemical species [114-116]. Microstreaming can also result, particularly if the bubble is not destroyed upon collapse and rebound. Probably the most thermally relevant aspect of intertial cavitation is the generation of broadband acoustic emissions upon collapse [99, 117]. Due to the frequency dependence of the absorption coefficient, high-frequency broadband noise emissions are readily absorbed by the surrounding tissue and converted into heat. In addition, these emissions provide a diagnostic tool for monitoring both the nature and extent of cavitation activity present in the HIFU field.

For exposure conditions relevant to HIFU, only bubbles smaller than about half the resonance size at the fundamental HIFU frequency will tend to behave inertially. Indeed, there exists an optimum size for which a bubble is most likely to undergo inertial growth and collapse [8]. Allen *et al.* showed that this size is essentially the nonlinear resonance radius of the driven bubble [118] and decreases with increasing HIFU pressure amplitude. For 1 MHz HIFU with 1 MPa pressure-amplitude in an aqueous medium, this optimum radius is approximately 0.06 μm.

Cavitation Nucleation in Tissue

Our discussion thus far has assumed that bubbles of adequate sizes pre-exist in a medium prior to being excited linearly or non-linearly by the incident HIFU field. In practice, adequate inhomogeneities must be present that will enable acoustically induced cavity nucleation upon exposure to ultrasound. These cavitation nuclei are typically pre-existing gas bodies or imperfectly wetted solids [101, 119]. In many aqueous systems, cavitation nuclei are plentiful, but it is not clear whether this is the case everywhere in human tissue. In

the absence of suitable nuclei, the pressure required to initiate cavitation can be so large (on the order of 10 MPa) that the ensuing bubble behavior rapidly grows out of control and deleterious biological effects result. Recent studies suggest that the targeted region can be populated with gas nuclei by injection of ultrasound contrast agents [120-125], which are stabilized microbubbles designed to enhance imaging contrast in blood [126-132]. A detailed discussion of acoustic cavitation nucleation mechanisms [1, 119, 133] and techniques [134-136] is beyond the scope of this paper. For the purposes of this discussion, we assume that some form of nucleating agent is present and cavitation can be both initiated and sustained at relatively modest HIFU pressure amplitudes on the order of 1-3 MPa.

Mechanisms of Cavitation-Enhanced Heating

HIFU-induced heating in tissue is directly dependent on the incident intensity and the local frequency-dependent absorption coefficient. As a result, stable and inertial cavitation will increase the rate at which acoustic energy is being converted into heat because they increase the length scales over which viscous absorption can occur, or redistribute some of the energy of the incident field as higher-frequency emissions that are more readily absorbed. The three primary mechanisms by which this enhanced heat deposition will occur – multiple scattering, absorption in the viscous boundary layer at the bubble wall and absorption of secondary acoustic emissions – are described in detail hereafter.

Whether bubbles are oscillating linearly or non-linearly, they will act as strong scatterers of the incident sound field. Multiple cavities contained within a volume of tissue will therefore effectively trap the incident acoustic energy, increasing the path length over which viscous absorption can occur within that region. Multiple scattering of the incident field will therefore result in enhanced heating over the volume of tissue containing bubbles.

Furthermore, the high shear stresses present in the boundary layer between an oscillating bubble and the surrounding medium will also lead to enhanced viscous absorption. Equation (2), which describes the bubble dynamics, includes a viscous stress term that is velocity-dependent and corresponds to the dissipative work done by the bubble on the surrounding medium. The bubble acts simultaneously as a vehicle for conversion of acoustic to mechanical energy, by virtue of the bubble dynamics, and from mechanical to thermal energy by virtue of viscous dissipation. An estimate of the cycle-averaged deposited power per bubble comes from consideration of the average rate of work done by viscous stress and is given by [99, 137]

$$D_{vis} = 16\pi\mu \left\langle \dot{R}^2 R \right\rangle_t \ . \tag{3}$$

This energy is dissipated solely as heat and depends on the shear viscosity μ of the medium, the equilibrium bubble size and the bubble dynamics.

When a bubble undergoes a violent collapse, the acceleration associated with its rebound is considerable and results in a very short burst of broadband sound. For micron and sub-micron bubbles pulsating inertially, this so-called secondary acoustic emission exceeds the HIFU energy scattered by the original bubble by orders of magnitude. The acoustic emission from a bubble undergoing volumetric pulsations is given by [99, 138]

$$p_{sae}(r,t) = \frac{\rho R}{r}\left(2\dot{R}^2 + R\ddot{R}\right)e^{-\alpha(r-R)} \ , \tag{4}$$

where r is radial distance from the center of the bubble and α is the frequency-dependent ultrasound attenuation coefficient for the medium. Two things are immediately obvious from Equation 4. First, since sound attenuation in tissue increases with increasing frequency, broadband emissions at high frequencies will be more readily absorbed than sound scattered

from the primary HIFU field at the fundamental frequency. Secondly, the amplitude of the emission is a strong function of both wall velocity and acceleration. The acceleration term can dominate in the case of inertial collapses, and is greatest at the point of maximum collapse.

At a distance *r*, the power emitted as secondary noise emissions is given by

$$W_{sae}(r) = 4\pi r^2 I(r) = \frac{4\pi r^2}{\rho c}\int_0^\infty p_{sae}^2 dt \quad , \tag{5}$$

where *I* is the acoustic intensity at the distance *r*. If the sound power emitted as secondary emissions at the surface of the bubble ($r = R$) is W_0, then the thermal power deposited in the volume subtended by r is given by:

$$D_{sae}(r) = W_o - W_{sae}(r) \quad . \tag{6}$$

It is evident from Equations 4–6 that bubbles radiating the most noise will be the bubbles that are most likely to contribute to heating through the absorption of radiated sound power.

The relative significance of cavitation-enhanced heating due to increased absorption in the viscous boundary layer near the bubble wall, described by Equation 3, and of that due to the absorption of secondary acoustic emissions, given by Equation 6, deserves further investigation. Direct simulations of the bubble response, as given by Equation 2, have been performed to compute the heat deposited by these two mechanisms [99, 139, 140]. The exact values of the shear viscosity and range of equilibrium bubble sizes are critically important to these calculations but are not known for biologically relevant media. Therefore, these simulations are set up as a parameter study in which the equilibrium bubble size was varied from 0.1 to 50 μm, and the shear viscosity was allowed to vary between one and hundred

times the shear viscosity of water (0.001 N-s/m^2.)

Results obtained for a 1 MHz HIFU exposure at a pressure amplitude of 2.8 MPa are shown in Figures 1a and 1b. Both plots reveal regions in which bubble-enhanced heating is maximal: Figure 1a shows maximum power depositions on the order of 50 mW, but only for the highest viscosities considered and for bubble sizes equal to, or somewhat larger than, the linear resonance radius of 3.72 μm. These larger bubbles are pulsating stably, and we conclude that, for these relatively low level HIFU exposure conditions, *stable cavitation is most effective at converting acoustical energy to heat via viscous loss*. Figure 1b shows that similar levels of heat deposition can be achieved by the absorption of secondary acoustic emissions, but this enhanced heating is associated with a broad range of sub-resonant bubble sizes and candidate media viscosities. Bubbles in this parameter range undergo inertial collapse, and from this we conclude that *inertial cavitation is more effective at converting acoustical energy to heat via the absorption of secondary acoustic emissions*.

Allowable Bubble Sizes in Tissue

The results of the simulations presented in Figure 1 suggest that both inertial and stable cavitation can induce comparable levels of enhanced heat deposition by different mechanisms, but for completely different ranges of equilibrium bubbles sizes. However, not all bubble sizes can necessarily exist in tissue under ultrasound exposure. Bubbles exposed to HIFU undergo a gradual growth in equilibrium size due to a process known as rectified diffusion [105, 106, 141-143] and, once they reach a critical radius, break up into smaller bubbles due to instabilities caused by surface perturbations. The specifics of these two processes are discussed in further detail by Yang [144] and Holt and Roy [99]. For now, it suffices to say that there exists an upper bound to allowable bubble sizes and bubbles smaller than this size undergo a cyclic process of growth followed by breakup, yielding an asymptotic bubble size

distribution that is limited at the lower end by surface tension and the upper end by surface instabilities.

For a given frequency and pressure amplitude, the range of allowable bubble sizes depends on both viscosity and dissolved gas concentration. For water-like viscosities and exposure conditions of 1 MHz and 2.5 MPa, the allowable size range is 10 nm – 1 μm [140, 144] irrespective of the dissolved gas concentration. For such conditions, only inertial cavities can exist, and bubble enhanced heating is due solely to the absorption of radiated noise. For viscosities greater than about 20 times that of water, the limiting bubble size distribution expands to 10 nm – 2 μm for a degassed medium (0.1% of saturation), and once again only inertial cavitation is supported. However, in a gas-saturated medium, the range becomes 10 nm – 18 μm. Both inertial and stable cavities can exist and contribute to heating, but only at the highest viscosities and dissolved gas concentrations.

It must be emphasized that the viscosities and gas concentrations encountered *in vivo* will vary with tissue type and physiological condition. Therefore, these numbers serve only as a qualitative guide of what one might expect to occur *in vivo.* Nevertheless, the modeling evidence suggests that, for most materials and for the relatively low level HIFU exposures under consideration, *bubble enhanced heating is most likely to result from the absorption of noise generated by inertial cavitation*. Thus we anticipate a correlation between a physical observable (noise) and a desired effect (heating). This testable hypothesis is investigated further in the context of experimental observations of cavitation-enhanced heating.

3. EXPERIMENTAL OBSERVATIONS OF CAVITATION-ENHANCED HEATING

Tissue-mimicking materials

There have been several investigations of the correlation between cavitation activity and the resulting rate of heating, both *in vivo* [82-84, 138, 145-148] and *in vitro* [81, 83, 84, 139]. In order to isolate the thermal effects due to cavitation and to develop techniques on how to best monitor and control the process, it is often desirable to carry out such experimentation under precisely known acoustic and thermal conditions in gel-based tissue-mimicking materials known as “tissue phantoms” [139, 149-151]. These media are generally designed to match at least some of the physical properties relevant to HIFU treatment in tissue, such as attenuation, density and speed of sound. However, it must be noted *a priori* that no phantom will provide an exact match to many other relevant tissue properties, such as the absorption coefficient, cavitation threshold, coefficient of non-linearity, or rate of tissue perfusion, and that such *in vitro* studies are primarily aimed at developing a qualitative rather than quantitative understanding of the cavitational and other mechanisms involved in tissue heating.

One commonly used tissue phantom consists of agar gel, graphite particles, and 1-proponol [139]. The 1-proponol is used to “tune” the sound speed of the phantom to match that of tissue. The graphite serves to introduce acoustic scatterers and thus enhances acoustic absorption. It can also provide nucleation sites for bubble formation. Indeed, the measured cavitation nucleation threshold for this material can be as low as 1.8 MPa, when saturated with gas. This is significantly less than thresholds reported in tissues, many of which exceed 4-6 MPa [1, 88-90]. The agar/graphite phantom is an ideal medium for promoting cavitation effects and monitoring HIFU-induced bubble behavior.

Cavitation Detection

A typical experimental setup used to investigate HIFU-induced cavitation and its associated heating effects is depicted in Figure 2. A single-element, 1.1 MHz, focused HIFU source (Sonic Concepts H-102 S/N-6) with a transmission aperture of 6 cm and a focal length of approximately 6 cm is driven using a sine-wave generator (Agilent 33250A) and power amplifier (ENI A150), and aimed at an agar-graphite tissue phantom. A needle hydrophone (not shown) can be embedded into the phantom to monitor the pressure field *in situ*. The HIFU half-power beam width is approximately 1 mm. Temperature is measured using a 125-µm diameter, bare-wire, Type-E thermocouple (not shown) positioned in the focal plane of the HIFU source and offset by approximately 0.5 mm with respect to the beam axis in order to reduce the possibility of cavitation occurring on the surface of the sensor.

A key element in the apparatus is a tightly focused broadband acoustic sensor (NDT-Panametrics V313-SU), of centre frequency 15 MHz, positioned at 90 degrees and confocally with the HIFU beam, the objective of which is to isolate, detect and monitor broadband noise emissions resulting from inertial cavitation activity at the focus of the HIFU transducer. The signal received by the 15-MHz transducer is amplified by 60 dB (EE&G 5185) and filtered through a passive 5-MHz high-pass filter (Allen Avionics F5081-5PO-B) to remove any contributions from the HIFU fundamental, second, third and fourth harmonic frequencies arising from nonlinear sound propagation. The resulting signal is attenuated by 6 dB using a passive in-line attenuator (JFW 50F-006) so as to match the full 1 V input range of a digitizing peak detector (G.E. Panametrics 5607). *This passive cavitation detection (PCD) scheme is therefore configured to sense broadband acoustic emissions from inertial cavitation, and not scattering from the primary HIFU beam from stable cavitation bubbles* [152, 153]. It is a real time indicator of the extent of inertial cavitation activity present within its sensing

volume, effectively defined by the focal region of the PCD transducer. Its output can be processed and displayed in real time, providing the user with a non-invasive "cavitation meter." It can also be stored and later correlated with measured temperature elevations and observations of lesion formation.

Correlation of observed heating with cavitation activity

Figure 3.I depicts the temperature elevation in an agar-graphite phantom following exposure of three different phantom locations to 1.1-MHz HIFU for 1 second at three different insonation amplitudes. Also plotted is the peak voltage from the PCD sampled in a 20 μsec window at a rate of 1000 samples/sec. At the lowest exposure pressure amplitude (1.65 MPa), the output of the PCD in Figure 3.I.c indicates that no inertial cavitation occurs in the confocal region of the HIFU and PCD transducers. A modest rate of heating is observed under those conditions, resulting in a temperature elevation of less than 10^{o} C during HIFU exposure, followed by cooling. This type of heating-cooling behaviour is well-predicted by a standard heat conduction model, commonly known as the bioheat transfer equation (BHTE) [99, 154]. The BHTE takes into account thermal conduction, has sink terms to account for tissue perfusion and convective blood cooling (both zero for this phantom), and a source term to incorporate energy deposition from ultrasound absorption. At these low pressures, no cavitation activity is evident and linear propagation effects alone account for the observed heating.

For a modest increase in HIFU pressure amplitude to 1.8 MPa, the heating rate initially observed in Figure 3.I.b differs only slightly from that seen in Figure 3.I.c. However, halfway through the HIFU exposure, there is a sudden and dramatic increase in heating coincident with an equally sudden and sustained burst of broadband emission. This strongly suggests that the origin of the enhanced heating phenomenon is related to the origin of acoustic

emissions: *inertial cavitation*.

Finally, an additional small increase in the HIFU insonation amplitude to 1.9 MPa results in the immediate onset of both inertial cavitation and enhanced heating, as shown in Figure 3.I.a. A temperature elevation of some 30^{o} C is obtained over the 1-second exposure and greatly exceeds that obtained without bubbles present. The temperature rise predicted by the BHTE at 1.8 MPa in the absence of cavitation should not exceed the increase at 1.65 MPa by more than 33%, yet the measured elevation is almost triple that at 1.65 MPa. In this phantom, and for these relatively low pressures, bubbles dominate the heating process.

The temperature rise observed over a wide range of HIFU excitation amplitudes deserves further investigation. Shown in Figure 3.II is the measured peak temperature elevation in the agar-graphite phantom exposed to 700-ms long tone bursts of high intensity focused ultrasound. Each data point represents an average of 5 measurements taken at a given HIFU pressure amplitude, and the phantom was allowed to cool for 100 seconds between measurements. The data suggests four distinct regions, presumably corresponding to differing regimes of bubble activity: linear heating, enhancement, saturation, and suppression.

As shown in Figure 3.I, the inertial cavitation threshold for this agar-graphite phantom is 1.8 MPa. At HIFU pressure amplitudes below that threshold, Figure 3.II shows that the temperature rise is quadratic with pressure, as predicted by the BHTE. As the pressure is increased beyond 1.8 MPa, the level of inertial cavitation activity gradually increases and coincides with a sudden and dramatic increase in the rate of heating, with peak temperature rises greatly in excess of those predicted by linear heating models in the absence of cavitation. However, further increases in the HIFU pressure amplitude beyond 2 MPa do not yield any further increase in the peak temperature reached. This is presumably due to gradual saturation

of the HIFU focal region with cavitation activity. For excitation pressures beyond some 3 MPa, the peak temperature recorded by the thermocouple suddenly decreases. At these relatively high HIFU pressures, it is likely that cavitation is initiated in the prefocal region as well as in the focal region: this will result in shielding of the original HIFU focus, due to increased attenuation through the prefocal bubble cloud, and will lead to enhanced heat deposition ahead of the intended focus. When bubbles and tissue heating are concerned, more power is not necessarily desirable, both in terms of heat deposition efficiency at the focus and the likelihood of generating unpredictably shaped and positioned lesions that extend well into the prefocal region.

It is important to note that these results were obtained in a gassy phantom that has a lower cavitation threshold and lower absorption coefficient than most tissues. As a result, it is much more susceptible to cavitation activity and will not get as hot as tissue during HIFU exposure. The relative contribution of cavitation-enhanced heating with respect to heating caused by absorption due to linear and non-linear sound propagation clearly depends on the relationship between the cavitation threshold pressure and that for which significant nonlinear propagation occurs. This has been investigated previously [83, 93-95, 155] and will not be addressed here. However, the effect of increasing temperature during HIFU exposure on cavitation-enhanced heating deserves further investigation and is discussed hereafter.

Role of ambient temperature

As tissue heats up during HIFU exposure, a number of significant changes take place. Proteins denature, leading to an increase in tissue stiffness and attenuation coefficient [156, 157]**.** The bubbles are stress-confined and may not be able to grow and collapse inertially [102]. This potentially important effect remains poorly understood and will not be discussed here.

However, what is known is that the hot tissue becomes supersaturated and proceeds to outgas into existing bubbles. The bubble equilibrium size increases and, in the process, existing cavities are less likely to grow and collapse inertially due to the mass loading of the surrounding tissue. Finally, the increasing temperature causes a significant increase in vapor pressure. As a result, the vapor inside the bubble is less likely to condense during the compression phase and serves to inhibit inertial collapse [158, 159] . The combined result of all these effects is a reduction in the bubble radial expansion ratio, defined as R_{max}/R_{min}. A decrease in the expansion ratio leads to a decrease in the broadband noise emissions following collapse and, by extension, to a reduction in the energy available for cavitation-enhanced HIFU heating [84, 160].

Calculations performed using the models described earlier (Equations 2-6) confirm this observation. For an air bubble in water, the thermal power deposited by secondary acoustic emssions and viscous boundary layer heating decreases by 50% and 60% respectively when the water temperature is increased from 20˚C to 90˚C [84]. This implies that, as the medium heats up, inertial cavitation bubbles cease to act as either thermal or broadband noise sources. At this point, a stable cavitation field in the form of acoustically driven boiling bubbles remains. However, visual observations suggest that these bubbles become very large and will therefore impact the local sound field primarily through acoustic scattering. For the reasons outlined in Section 2, sound scattering from boiling cavitation at the focus enhances pre-focal heating. This effect is undesirable, as it can lead to the generation of malformed “tadpole-shaped” lesions of unpredictable shape, size and position. However, boiling bubbles are sufficiently large that they become clearly visible as a bright region in diagnostic ultrasound pulse-echo images of the treatment volume. This increased echogenicity has proven beneficial for treatment monitoring and guidance using diagnostic ultrasound. [73, 90,

161-164]

4. MONITORING AND CONTROL OF CAVITATION DURING HIFU

In the previous section, we demonstrated that at relatively modest HIFU excitation amplitudes and at sub-boiling temperatures, inertial cavitation can greatly enhance the rate of heating and provides a mechanism for increased heat deposition efficiency at the focus. However, the rapidly changing conditions and increasing temperature during HIFU exposure have also been shown to impact the bubble dynamics and their resulting heating enhancement, leading to potentially undesirable pre-focal effects. This emphasizes the need for adequate monitoring and control of inertial cavitation activity during HIFU exposure, if it is to be harnessed for optimal treatment delivery.

Cavitation Monitoring

HIFU therapy is often delivered under ultrasound guidance, utilizing linear phased-arrays driven in pulse-echo mode to image the HIFU focal region. Previous investigators have suggested that relatively subtle grayscale changes in such ultrasound images during HIFU exposure could provide a direct indication of inertial cavitation activity . To investigate this hypothesis, an agar-graphite tissue phantom was exposed to 1.1-MHz HIFU, whilst cavitation activity at the focus was monitored simultaneously using the previously described passive cavitation detector (PCD) and a 5-MHz ultrasound imager, as depicted in Figure 2. The PCD signal was fed directly to an 8-bit peak detector with a 20-μs detection window, the output of which was transferred digitally to a 12-bit DAQ board (AT-MIO-16E-1, National Instruments) on a PC and displayed as a function of time. The peak detector also passed the raw PCD signal to a 10 MHz vector signal analyzer (89410A, Hewlett-Packard), which

displays the frequency spectrum of the received PCD signal in real time. The imaging scan head (Analogic Corp. 8802) is a 192-element array with bandwidth 3.5-6 MHz, driven by an Analogic engine in pulse-echo mode. The S-video output from the engine was fed directly to an S-Video ADC on the PC, as well as recorded using an S-VHS VCR.

A B-mode image of the HIFU focal region prior to exposure is shown in Figure 4, where the confocal region of the HIFU and PCD transducers is denoted by the white cross. The HIFU pressure amplitude was ramped up in steps of 0.15 MPa, as shown on the top axis of Figure 4, every five seconds, as indicated on the bottom axis of Figure 4. At the end of the 5-second interval for which a new HIFU excitation amplitude had been imposed, the HIFU field was switched off and the B-mode image was visually examined for the appearance of a noticeable hyperechogenic region. If none were identified, the confocal position of the HIFU, PCD and imaging transducers was moved to a different location in the phantom, whilst maintaining the propagation path length to each transducer constant. The HIFU amplitude was then ramped up again from zero in five-second intervals until the next highest excitation amplitude increment was reached, and the procedure was repeated until a hyperechogenic region became visible on the B-mode image.

Such a region became visible for the first time following 45 seconds of HIFU exposure, by the end of which the HIFU amplitude had been ramped up every 5 seconds in 0.15-MPa increments to 1.35 MPa. The resulting B-mode image, shown in Figure 4 at t = 46 seconds, shows a clearly visible bright-up that is coincident with the confocal region of the HIFU, PCD and imaging transducers (indicated by the white cross). However, closer investigation of the peak value and spectral content of the PCD signal over the 45 second exposure, also plotted in Figure 4, strongly suggests that inertial cavitation activity had been initiated as

early as t = 20 s, when the HIFU pressure amplitude was 0.9 MPa. The spectral content of the PCD signal further confirms this, by exhibiting a clear jump in broadband noise emissions between t = 16 s and t = 31 s. In the time interval between t = 20 s and t = 45 seconds, both the PCD peak value and spectral content indicate that the level of inertial cavitation activity continues to increase and is sustained throughout the exposure, yet a hyperechogenic region does not become visible until a pressure amplitude of 1.35 MPa is reached and maintained for five seconds until t = 45 s.

From this, we conclude that the appearance of a hyperechogenic region on B-mode images constitutes neither a necessary nor a sufficient condition for inertial cavitation to have occurred during HIFU exposure [165]. As suggested in the previous section, the appearance of a hyperechogenic region is most likely linked to the formation of large, boiling cavities as the temperature is increased by exposure to HIFU. Similar observations have been reported during experimentation *in vivo* by other investigators [90, 161, 166]. In general, a Passive Cavitation Detection scheme constitutes the most reliable, cost-effective and sensitive means of real-time cavitation detection during HIFU exposure. However, when targeting deep-seated organs such as the liver or kidney with HIFU, the large ultrasound propagation path could make high-frequency secondary acoustic emissions difficult to detect. Many challenges remain in order to develop truly clinically applicable, reliable means of passive cavitation detection.

Control of Inertial Cavitation

As discussed in Section 3, at relatively high HIFU excitation amplitudes inertial cavitation activity can migrate out of the focal region towards the HIFU transducer, leading to undesirable prefocal damage and shielding of the original focus. Potential evidence of this is shown in Figure 5, where the rms voltage detected by the PCD during 2.89 MPa HIFU

exposure of an agar-graphite phantom is shown to decay rapidly during continuous-wave (CW) excitation, suggesting that the bubble cloud is migrating towards the HIFU transducer and out of the field of view of the PCD. It must be noted that some of the observed decrease could also be due to the effect of increasing ambient temperature, as discussed earlier. However, Figure 5 shows that switching to a 20% duty cycle following 1 second of CW HIFU excitation, as previously suggested [167], can help sustain the level of inertial cavitation activity throughout the HIFU exposure. Three particular implementations of a 20% duty cycle following 1 second of HIFU excitation are investigated here, using a 5, 10 and 100-cycle on-time, and the results suggest that shorter pulses are more effective at preventing shielding of the original focus than longer pulses.

Such schemes for controlling inertial cavitation [167-173] may well play a crucial role in future attempts to harness cavitation-enhanced heating for optimal treatment delivery. However, it must be noted that, during 20% duty cycle excitation, only one fifth of the power delivered during CW exposure is received at the focus. The impact that this has on the resulting rate of heating needs to be investigated further, as does the effect of varying other parameters such as HIFU frequency and excitation amplitude in real-time.

5. CONCLUSION

Cavitation has tremendous potential to enhance the rate of heating and to improve the spatial localization of heat deposition during HIFU treatment. Under exposure conditions relevant to HIFU therapy, it has been shown that most of this enhancement is due to the re-radiation of the incident sound field as broadband noise emissions by inertially cavitating bubbles, whilst scattering and viscous absorption in the bubble boundary layer play a relatively minor role. However, as the ambient temperature is increased and the properties of tissue change, inertial

cavitation gradually shuts down and can give rise to larger, boiling cavities that play a significant thermal role through scattering. These boiling cavities currently play a useful role in monitoring HIFU therapy, as they are readily visible on B-mode ultrasound images, but could also be indicative of over-treatment of the target region. New means of monitoring and controlling inertial cavitation activity are being proposed, which could be used to exploit the enhanced heating, treatment localization and treatment monitoring advantages that could be provided by inertially cavitating microbubbles. The behaviour of such microbubbles in temperature-varying viscoelastic media is still poorly understood, and many challenges remain in terms of developing truly clinically relevant means of monitoring and controlling inertial cavitation activity. However, it is hoped that, in due course, these challenges can be overcome and give rise to a novel, efficacious, cavitation-based HIFU therapy system.

6. ACKNOWLEDGEMENTS

The authors would like to acknowledge the efforts of students and colleagues whose work is featured in this article: Patrick Edson, R. Glynn Holt, Charles Thomas, Jamie R.T. Collin and Adam Muckle. Authors Roy and Farny would like to acknowledge generous financial support of their primary research sponsors: the United States Army (award number DAMD17-02-2-0014, for which The U.S. Army Medical Research Acquisition Activity, 820 Chandler Street, Fort Detrick, MD is the awarding and administering acquisition office), and the Center for Subsurface Sensing and Imaging Systems (funded under the Engineering Research Centers Program of the National Science Foundation; award number EEC-9986821). Dr. Coussios' work in this area has been in part supported by the F.V. Hunt Post-Doctoral Fellowship of the Acoustical Society of America. Finally, both Dr Coussios and Dr ter Haar would like to acknowledge the generous ongoing support of the UK's Engineering and Physical Sciences Research Council.

REFERENCES

[1]Church CC. Spontaneous homogeneous nucleation, inertial cavitation and the safety of diagnostic ultrasound. Ultrasound in Medicine and Biology. 2002 Oct;28(10):1349-64.

[2]Miller MW, Everbach EC, Miller WM, Battaglia LF. Biological and environmental factors affecting ultrasound-induced hemolysis in vitro: 2. Medium dissolved gas (pO(2)) content. Ultrasound in Medicine and Biology. 2003 Jan;29(1):93-102.

[3]Apfel RE. ACOUSTIC CAVITATION SERIES .4. ACOUSTIC CAVITATION INCEPTION. Ultrasonics. 1984;22(4):167-73.

[4]Neppiras EA. Acoustic cavitation. Physics Reports. 1980;61(3):159-251.

[5]Apfel RE. Acoustic cavitation. Ultrasonics. 1981:355-411.

[6]Apfel RE. Acoustic cavitation prediction. The Journal of the Acoustical Society of America. 1981;69:1624.

[7]Crum LA, Fowlkes JB. ACOUSTIC CAVITATION GENERATED BY MICROSECOND PULSES OF ULTRASOUND. Nature. 1986 Jan;319(6048):52-4.

[8]Holland CK, Apfel RE. THRESHOLDS FOR TRANSIENT CAVITATION PRODUCED BY PULSED ULTRASOUND IN A CONTROLLED NUCLEI ENVIRONMENT. Journal of the Acoustical Society of America. 1990 Nov;88(5):2059-69.

[9]Miller DL. ACOUSTIC CAVITATION SERIES .6. GAS BODY ACTIVATION. Ultrasonics. 1984;22(6):261-9.

[10] Miller DL. A REVIEW OF THE ULTRASONIC BIOEFFECTS OF MICROSONATION, GAS-BODY ACTIVATION, AND RELATED CAVITATION-LIKE PHENOMENA. Ultrasound in Medicine and Biology. 1987 Aug;13(8):443-70.

[11] Miller DL. UPDATE ON SAFETY OF DIAGNOSTIC ULTRASONOGRAPHY. Journal of Clinical Ultrasound. 1991 Nov-Dec;19(9):531-40.

[12] Cardinale A, Lagalla R, Giambanco V, Aragona F. Bioeffects of ultrasound: an experimental study on human embryos. Ultrasonics. 1991;29(3):261-3.

[13] Holland CK, Deng CX, Apfel RE, Alderman JL, Fernandez LA, Taylor KJW. Direct evidence of cavitation in vivo from diagnostic ultrasound. Ultrasound in Medicine and Biology. 1996;22(7):917-25.

[14] Miller MW, Miller DL, Brayman AA. A review of in vitro bioeffects of inertial ultrasonic cavitation from a mechanistic perspective. Ultrasound in Medicine and Biology. 1996;22(9):1131-54.

[15] Barnett SB, ter Haar GR, Ziskin MC, Rott HD, Duck FA, Maeda K. International recommendations and guidelines for the safe use of diagnostic ultrasound in medicine. Ultrasound in Medicine and Biology. 2000 Mar;26(3):355-66.

[16] Fowlkes JB, Holland CK. Mechanical bioeffects from diagnostic ultrasound: AIUM consensus statements - Introduction. Journal of Ultrasound in Medicine. 2000 Feb;19(2):69-72.

[17] Holland CK, Roy RA, Biddinger PW, Disimile CJ, Cawood C. Cavitation mediated rat lung bioeffects from diagnostic ultrasound. The Journal of the Acoustical Society of America. 2001;109:2433.

[18] Fowlkes JB. Ultrasound bioeffects and NCRP on needed US exposures: The status of current output limits and displays. Medical Physics. 2002 Jun;29(6):1282-.

[19] Holland CK, Apfel RE. AN IMPROVED THEORY FOR THE PREDICTION OF MICROCAVITATION THRESHOLDS. Ieee Transactions on Ultrasonics Ferroelectrics and Frequency Control. 1989 Mar;36(2):204-8.

[20] Apfel RE, Holland CK. GAUGING THE LIKELIHOOD OF CAVITATION FROM SHORT-PULSE, LOW-DUTY CYCLE DIAGNOSTIC ULTRASOUND. Ultrasound in Medicine and Biology. 1991;17(2):179-85.

[21] Church CC. Frequency, pulse length, and the mechanical index. Acoustics Research Letters Online-Arlo. 2005 Jul;6(3):162-8.

[22] Fowlkes JB, Holland CK. Mechanical bioeffects from diagnostic ultrasound: AIUM consensus statements. American Institute of Ultrasound in Medicine. J Ultrasound Med. 2000;19(2):69-72.

[23] Vaezy S, Martin R, Schmiedl U, Caps M, Taylor S, Beach K, et al. Liver hemostasis using high-intensity focused ultrasound. Ultrasound in Medicine and Biology. 1997;23(9):1413-20.

[24] Vaezy S, Martin R, Yaziji H, Kaczkowski P, Keilman G, Carter S, et al. Hemostasis of punctured blood vessels using high-intensity focused ultrasound. Ultrasound in Medicine and Biology. 1998 Jul;24(6):903-10.

[25] Martin RW, Vaezy S, Kaczkowski P, Keilman G, Carter S, Caps M, et al. Hemostasis of punctured vessels using Doppler-guided high-intensity ultrasound. Ultrasound in Medicine and Biology. 1999 Jul;25(6):985-90.

[26] Vaezy S, Martin R, Kaczkowski P, Keilman G, Goldman B, Yaziji H, et al. Use of high-intensity focused ultrasound to control bleeding. Journal of Vascular Surgery. 1999 Mar;29(3):533-42.

[27] Poliachik SL, Chandler WL, Mourad PD, Ollos RJ, Crum LA. Activation, aggregation and adhesion of platelets exposed to high-intensity focused ultrasound. Ultrasound in Medicine and Biology. 2001 Nov;27(11):1567-76.

[28] Vaezy S, Martin R, Crum L. High intensity focused ultrasound: A method of hemostasis. Echocardiography-a Journal of Cardiovascular Ultrasound and Allied Techniques. 2001 May;18(4):309-15.

[29] Hwang JH, Kimmey M, Martin R, Vaezy S. Acoustic hemostasis of lacerated veins: Potential applications for gastrointestinal bleeding. Gastrointestinal Endoscopy. 2002 Apr;55(5):AB108-AB.

[30] Vaezy S, Noble ML, Keshavarzi A, Paun M, Prokop AF, Cornejo C, et al. Liver hemostasis with high-intensity ultrasound - Repair and healing. Journal of Ultrasound in Medicine. 2004 Feb;23(2):217-25.

[31] Vaezy S, Vaezy S, Starr F, Chi E, Cornejo C, Crum L, et al. Intra-operative acoustic hemostasis of liver: production of a homogenate for effective treatment. Ultrasonics. 2005 Feb;43(4):265-9.

[32] Zderic V, Keshavarzi A, Noble ML, Paun M, Sharar SR, Crum LA, et al. Hemorrhage control in arteries using high-intensity focused ultrasound: A survival study. Ultrasonics. 2006 Jan;44(1):46-53.

[33] Rivens IH, Rowland I, Denbow M, Fisk NM, Leach MO, ter Haar GR. Focused ultrasound surgery-induced vascular occlusion in fetal medicine. Proceedings of SPIE. 2003;3249:260.

[34] Denbow ML, Rivens IH, Rowland IJ, Leach MO, Fisk NM, ter Haar GR. Preclinical

development of noninvasive vascular occlusion with focused ultrasonic surgery for fetal therapy. American Journal of Obstetrics and Gynecology. 2000 Feb;182(2):387-92.

[35] Trubestein G, Engel C, Etzel F, Sobbe A, Cremer H, Stumpff U. Thrombolysis by ultrasound. Clin Sci Mol Med Suppl. 1976;3:697s-8s.

[36] Lauer CG, Burge R, Tang DB, Bass BG, Gomez ER, Alving BM. Effect of ultrasound on tissue-type plasminogen activator-induced thrombolysis. Circulation. 1992;86(4):1257-64.

[37] Luo H, Steffen W, Cercek B, Arunasalam S, Maurer G, Siegel RJ. Enhancement of thrombolysis by external ultrasound. Am Heart J. 1993;125(6):1564-9.

[38] Sehgal CM, Leveen RF, Shlansky-Goldberg RD. Ultrasound-assisted thrombolysis. Invest Radiol. 1993;28(10):939-43.

[39] Olsson SB, Johansson B, Nilsson AM, Olsson C, Roijer A. Enhancement of thrombolysis by ultrasound. Ultrasound Med Biol. 1994;20(4):375-82.

[40] Kornowski R, Meltzer RS, Chernine A, Vered Z, Battler A. Does external ultrasound accelerate thrombolysis? Results from a rabbit model. Circulation. 1994;89(1):339-44.

[41] Shlansky-Goldberg RD. Catheter-delivered ultrasound potentiates in vitro thrombolysis. Soc Intervent Radiol 1996.

[42] Hamm CW, Steffen W, Terres W, de Scheerder I, Reimers J, Cumberland D, et al. Intravascular therapeutic ultrasound thrombolysis in acute myocardial infarctions. Am J Cardiol. 1997;80(2):200-4.

[43] Tachibana K. Prototype therapeutic ultrasound emitting catheter for accelerating thrombolysis. Am inst Ulrrasound Med 1997.

[44] Porter TR, Kricsfeld D, Lof J, Everbach EC, Xie F. Effectiveness of transcranial and transthoracic ultrasound and microbubbles in dissolving intravascular thrombi. Journal of Ultrasound in Medicine. 2001 Dec;20(12):1313-25.

[45] Shaw GJ, Meunier JM, Cheng JY, Holland CK. Duty cycle dependence of ultrasound enhanced thrombolysis in an in-vitro human clot model. Annals of Emergency Medicine. 2005 Sep;46(3):S27-S.

[46] Parikh DS, Tiukinhoy-Laing S, Huang SL, Holland CK, MacDonald RC, McPherson DD, et al. Targeting of tissue plasminogen activator-loaded echogenic liposomes for site-specific thrombolysis. Arteriosclerosis Thrombosis and Vascular Biology. 2006 May;26(5):E102-E.

[47] Tata DB, Biglow J, Wu J, Tritton TR, Dunn F. Ultrasound-enhanced hydroxyl radical production from two clinically employed anti-cancer drugs, adriamycin and mitomycin C. Ultrasonics Sonochemistry. 1996;3(1):39-45.

[48] Umemura SI, Yumita N, Nishigaki R, Umemura K. Sonochemical activation of hematoporphyrin: a potential modalityfor cancer treatment. Ultrasonics Symposium, 1989 Proceedings, IEEE 1989. 1989:955-60.

[49] Jeffers J, Feng RQ, Fowlkes JB, Brenner DE, Cain CA. Sonodynamic therapy: activation of anticancer agents withultrasound. Ultrasonics Symposium, 1991 Proceedings, IEEE 1991. 1991:1367-70.

[50] Miyoshi N, Misik V, Fukuda M, Riesz P. Effect of gallium-porphyrin analogue ATX-70 on nitroxide formation from a cyclic secondary amine by ultrasound: on the mechanism of sonodynamic activation. Radiat Res. 1995;143(2):194-202.

[51] Hynynen K, McDannold N, Vykhodtseva N, Jolesz FA. Noninvasive MR

imaging-guided focal opening of the blood-brain barrier in rabbits. Radiology. 2001 Sep;220(3):640-6.

[52] Mesiwala AH, Farrell L, Wenzel HJ, Silbergeld DL, Crum LA, Winn HR, et al. High-intensity focused ultrasound selectively disrupts the blood-brain barrier in vivo. Ultrasound in Medicine and Biology. 2002 Mar;28(3):389-400.

[53] Hynynen K, McDannold N, Martin H, Jolesz FA, Vykhodtseva N. The threshold for brain damage in rabbits induced by bursts of ultrasound in the presence of an ultrasound contrast agent (Optison (R)). Ultrasound in Medicine and Biology. 2003;29(3):473-81.

[54] McDannold N, Vykhodtseva N, Jolesz FA, Hynynen K. MRI investigation of the threshold for thermally induced blood-brain barrier disruption and brain tissue damage in the rabbit brain. Magnetic Resonance in Medicine. 2004 May;51(5):913-23.

[55] Sheikov N, McDannold N, Vykhodtseva N, Jolesz F, Hynynen K. Cellular mechanisms of the blood-brain barrier opening induced by ultrasound in presence of microbubbles. Ultrasound in Medicine and Biology. 2004 Jul;30(7):979-89.

[56] Hynynen K, McDannold N, Sheikov NA, Jolesz FA, Vykhodtseva N. Local and reversible blood-brain barrier disruption by noninvasive focused ultrasound at frequencies suitable for trans-skull sonications. Neuroimage. 2005 Jan;24(1):12-20.

[57] McDannold N, Vykhodtseva N, Raymond S, Jolesz FA, Hynynen K. MRI-guided targeted blood-brain barrier disruption with focused ultrasound: Histological findings in rabbits. Ultrasound in Medicine and Biology. 2005 Nov;31(11):1527-37.

[58] Hynynen K, McDannold N, Vykhodtseva N, Raymond S, Weissleder R, Jolesz FA, et al. Focal disruption of the blood-brain barrier due to 260-kHz ultrasound bursts: a method for molecular imaging and targeted drug delivery. Journal of Neurosurgery. 2006 Sep;105(3):445-54.

[59] Kinoshita M, McDannold N, Jolesz FA, Hynynen K. Noninvasive localized delivery of Herceptin to the mouse brain by MRI-guided focused ultrasound-induced blood-brain barrier disruption. Proceedings of the National Academy of Sciences of the United States of America. 2006 Aug;103(31):11719-23.

[60] Kinoshita M, McDannold N, Jolesz FA, Hynynen K. Targeted delivery of antibodies through the blood-brain barrier by MRI-guided focused ultrasound. Biochemical and Biophysical Research Communications. 2006 Feb;340(4):1085-90.

[61] McDannold N, Vykhodtseva N, Hynynen K. Targeted disruption of the blood-brain barrier with focused ultrasound: association with cavitation activity. Physics in Medicine and Biology. 2006 Feb;51(4):793-807.

[62] Bao SP, Thrall BD, Miller DL. Transfection of a reporter plasmid into cultured cells by sonoporation in vitro. Ultrasound in Medicine and Biology. 1997;23(6):953-9.

[63] Miller DL, Bao SP, Gies RA, Thrall BD. Ultrasonic enhancement of gene transfection in murine melanoma tumors. Ultrasound in Medicine and Biology. 1999 Nov;25(9):1425-30.

[64] Miller DL, Dou CY, Song JM. DNA transfer and cell killing in epidermoid cells by diagnostic ultrasound activation of contrast agent gas bodies in vitro. Ultrasound in Medicine and Biology. 2003 Apr;29(4):601-7.

[65] Everbach EC, Francis CW. Cavitational mechanisms in ultrasound-accelerated thrombolysis at 1 MHz. Ultrasound in Medicine and Biology. 2000 Sep;26(7):1153-60.

[66] Datta S, Coussios CC, McAdory LE, Tan J, Porter T, De Courten-Myers G, et al. Correlation of cavitation with ultrasound enhancement of thrombolysis. Ultrasound in

Medicine and Biology. 2006 Aug;32(8):1257-67.

[67] Miller DL, Pislaru SV, Greenleaf JF. Sonoporation: Mechanical DNA Delivery by Ultrasonic Cavitation. Somatic Cell and Molecular Genetics. 2002;27(1):115-34.

[68] Ohl CD, Arora M, Ikink R, de Jong N, Versluis M, Delius M, et al. Sonoporation from jetting cavitation bubbles. Biophysical Journal. 2006 Dec;91(11):4285-95.

[69] Wu J. A possible physical mechanism of ultrasound-activated gene delivery: Shear stress generated by microstreaming. The Journal of the Acoustical Society of America. 2001;110:2668.

[70] Fry WJ, Fry RB. Temperature Changes Produced in Tissue during Ultrasonic Irradiation. The Journal of the Acoustical Society of America. 1953;25:6.

[71] Jw B, Wj FRY, Fj FRY, Rf K. Effects of high intensity ultrasound on the central nervous system of the cat. J Comp Neurol. 1955;103(3):459-84.

[72] Wj FRY, Wh Jr M, Jw B, Fj FRY. Production of focal destructive lesions in the central nervous system with ultrasound. J Neurosurg. 1954;11(5):471-8.

[73] Kennedy JE. High-intensity focused ultrasound in the treatment of solid tumours. Nat Rev Cancer. 2005;5(4):321-7.

[74] Rooney JA, Gammell PM, Hestenes JD, Chin HP, Blankenhorn DH. VELOCITY AND ATTENUATION OF SOUND IN ARTERIAL TISSUES. Journal of the Acoustical Society of America. 1982;71(2):462-6.

[75] Parker KJ. Ultrasonic attenuation and absorption in liver tissue. Ultrasound Med Biol. 1983;9(4):363-9.

[76] Hill CR, Bamber JC, Haar GR. Physical Principles of Medical Ultrasonics: John Wiley & Sons 2004.

[77] Chivers RC, Hill CR. Ultrasonic attenuation in human tissue. Ultrasound in Medicine & Biology. 1975;2(1):25-9.

[78] Hynynen K, Watmough DJ, Mallard JR. DESIGN OF ULTRASONIC TRANSDUCERS FOR LOCAL HYPERTHERMIA. Ultrasound in Medicine and Biology. 1981;7(4):397-402.

[79] Hill CR. Optimum acoustic frequency for focused ultrasound surgery. Ultrasound in Medicine & Biology. 1994;20(3):271-7.

[80] Hynynen K. THE THRESHOLD FOR THERMALLY SIGNIFICANT CAVITATION IN DOG THIGH MUSCLE INVIVO. Ultrasound in Medicine and Biology. 1991;17(2):157-69.

[81] Holt RG, Roy RA. Measurements of bubble-enhanced heating from focused, MHz-frequency ultrasound in a tissue-mimicking material. Ultrasound in Medicine and Biology. 2001 Oct;27(10):1399-412.

[82] Miller DL, Gies RA. The interaction of ultrasonic heating and cavitation in vascular bioeffects on mouse intestine. Ultrasound in Medicine and Biology. 1998 Jan;24(1):123-8.

[83] Chen WS, Lafon C, Matula TJ, Vaezy S, Crum LA. Mechanisms of lesion formation in high intensity focused ultrasound therapy. Acoustics Research Letters Online-Arlo. 2003 Apr;4(2):41-6.

[84] Farny CH. Identifying and monitoring the roles of cavitation in heating from high intensity focussed ultrasound. Boston: Boston University; 2006.

[85] Leighton TG. The Acoustic Bubble: Academic Press 1994.

[86] Mellen RH. Ultrasonic Spectrum of Cavitation Noise in Water. The Journal of the Acoustical Society of America. 1954;26:356.

[87] Holt RG, Crum LA. ACOUSTICALLY FORCED-OSCILLATIONS OF AIR BUBBLES IN WATER - EXPERIMENTAL RESULTS. Journal of the Acoustical Society of America. 1992 Apr;91(4):1924-32.

[88] Hynynen K. THE ROLE OF NONLINEAR ULTRASOUND PROPAGATION DURING HYPERTHERMIA TREATMENTS. Medical Physics. 1991 Nov-Dec;18(6):1156-63.

[89] Yang X, Church CC. A model for the dynamics of gas bubbles in soft tissue. The Journal of the Acoustical Society of America. 2005;118(6):3595-606.

[90] Rabkin BA, Zderic V, Vaezy S. Hyperecho in ultrasound images of HIFU therapy: Involvement of cavitation. Ultrasound in Medicine and Biology. 2005 Jul;31(7):947-56.

[91] Damianou C, Hynynen K. THE EFFECT OF VARIOUS PHYSICAL PARAMETERS ON THE SIZE AND SHAPE OF NECROSED TISSUE VOLUME DURING ULTRASOUND SURGERY. Journal of the Acoustical Society of America. 1994 Mar;95(3):1641-9.

[92] Damianou CA, Hynynen K, Fan XB. EVALUATION OF ACCURACY OF A THEORETICAL-MODEL FOR PREDICTING THE NECROSED TISSUE VOLUME DURING FOCUSED ULTRASOUND SURGERY. Ieee Transactions on Ultrasonics Ferroelectrics and Frequency Control. 1995 Mar;42(2):182-7.

[93] Meaney PM, Cahill MD, ter Haar GR. The intensity dependence of lesion position shift during focused ultrasound surgery. Ultrasound in Medicine and Biology. 2000 Mar;26(3):441-50.

[94] Bailey MR, Couret LN, Sapozhnikov OA, Khokhlova VA, ter Haar G, Vaezy S, et al. Use of overpressure to assess the role of bubbles in focused ultrasound lesion shape in vitro. Ultrasound in Medicine and Biology. 2001 May;27(5):695-708.

[95] Khokhlova VA, Bailey MR, Reed JA, Cunitz BW, Kaczkowski PJ, Crum LA. Effects of nonlinear propagation, cavitation, and boiling in lesion formation by high intensity focused ultrasound in a gel phantom. Journal of the Acoustical Society of America. 2006 Mar;119(3):1834-48.

[96] Prosperetti A. THERMAL EFFECTS AND DAMPING MECHANISMS IN FORCED RADIAL OSCILLATIONS OF GAS-BUBBLES IN LIQUIDS. Journal of the Acoustical Society of America. 1977;61(1):17-27.

[97] Prosperetti A. ACOUSTIC CAVITATION SERIES .2. BUBBLE PHENOMENA IN SOUND FIELDS .1. Ultrasonics. 1984;22(2):69-78.

[98] Minnaert M. On musical air bubbles and the sounds of running water. Philos Mag. 1933;16(7):235.

[99] Holt RG, Roy RA. Bubble dynamics in therapeutic ultrasound. In: Dionikov A, ed. *Bubble and particle dynamics in acoustic fields: : modern trends and applications*. Kerala: Transworld Research Network 2005:108-229.

[100] Prosperetti A. ACOUSTIC CAVITATION SERIES .3. BUBBLE PHENOMENA IN SOUND FIELDS .2. Ultrasonics. 1984;22(3):115-24.

[101] Apfel RE. Acoustic Cavitation, Methods Expt. Physics (ed PD Edmonds).

1981;19:355–411.

[102] Yang XM, Church CC. A simple viscoelastic model for soft tissues in the frequency range 6-20 MHz. Ieee Transactions on Ultrasonics Ferroelectrics and Frequency Control. 2006 Aug;53(8):1404-11.

[103] Keller JB, Miksis M. Bubble oscillations of large amplitude. The Journal of the Acoustical Society of America. 1980;68:628.

[104] Prosperetti A, Lezzi A. BUBBLE DYNAMICS IN A COMPRESSIBLE LIQUID .1. 1ST-ORDER THEORY. Journal of Fluid Mechanics. 1986 Jul;168:457-78.

[105] Crum LA, Hansen GM. GENERALIZED EQUATIONS FOR RECTIFIED DIFFUSION. Journal of the Acoustical Society of America. 1982;72(5):1586-92.

[106] Church CC. PREDICTION OF RECTIFIED DIFFUSION DURING NONLINEAR BUBBLE PULSATIONS AT BIOMEDICAL FREQUENCIES. Journal of the Acoustical Society of America. 1988 Jun;83(6):2210-7.

[107]Elder SA. Cavitation Microstreaming. The Journal of the Acoustical Society of America. 1959;31:54.

[108] Nyborg WL. Acoustic streaming. Physical Acoustics. 1965;2(B):65-331.

[109] Miller DL. Particle gathering and microstreaming near ultrasonically activated gas-filled micropores. The Journal of the Acoustical Society of America. 1988;84:1378.

[110] Wu J, Du G. Streaming generated by a bubble in an ultrasound field. The Journal of the Acoustical Society of America. 1997;101:1899.

[111] Rooney JA. ACOUSTIC STREAMING AS A MECHANISM IN TREATMENT OF SUSPENSIONS. Journal of the Acoustical Society of America. 1970;48(1):114-&.

[112] Rooney JA. HEMOLYSIS NEAR AN ULTRASONICALLY PULSATING GAS BUBBLE. Science. 1970;169(3948):869-&.

[113] Williams AR. DISORGANIZATION AND DISRUPTION OF MAMMALIAN AND AMOEBOID CELLS BY ACOUSTIC MICROSTREAMING. Journal of the Acoustical Society of America. 1972;52(2):688-&.

[114] Harvey EN. Sonoluminescence and Sonic Chemiluminescence. Journal of the American Chemical Society. 1939;61(9):2392-8.

[115] Suslick KS. SONOCHEMISTRY. Science. 1990 Mar;247(4949):1439-45.

[116] Roy RA. PHYSICAL ASPECTS OF SONOLUMINESCENCE FROM ACOUSTIC CAVITATION. Ultrasonics Sonochemistry. 1994 Mar;1(1):S5-S8.

[117] Hilgenfeldt S, Lohse D. The acoustics of diagnostic microbubbles: dissipative effects and heat deposition. Ultrasonics. 2000 Mar;38(1-8):99-104.

[118] Allen JS, Roy RA, Church CC. On the role of shear viscosity in mediating inertial cavitation from short-pulse, megahertz-frequency ultrasound. Ieee Transactions on Ultrasonics Ferroelectrics and Frequency Control. 1997 Jul;44(4):743-51.

[119] Atchley AA, Prosperetti A. THE CREVICE MODEL OF BUBBLE NUCLEATION. Journal of the Acoustical Society of America. 1989 Sep;86(3):1065-84.

[120] Yu T, Wang G, Hu K, Ma P, Bai J, Wang Z. A microbubble agent improves the therapeutic efficiency of high intensity focused ultrasound: a rabbit kidney study. Urological Research. 2004;32(1):14-9.

[121] Umemura S, Kawabata K, Sasaki K. In vivo acceleration of ultrasonic tissue heating by

microbubble agent. Ultrasonics, Ferroelectrics and Frequency Control, IEEE Transactions on. 2005;52(10):1690-8.

[122] Kaneko Y, Maruyama T, Takegami K, Watanabe T, Mitsui H, Hanajiri K, et al. Use of a microbubble agent to increase the effects of high intensity focused ultrasound on liver tissue. European Radiology. 2005;15(7):1415-20.

[123] McDannold NJ, Vykhodtseva NI, Hynynen K. Microbubble contrast agent with focused ultrasound to create brain lesions at low power levels: MR imaging and histologic study in rabbits. Radiology. 2006 Oct;241(1):95-106.

[124] Apfel RE. VAPOR NUCLEATION AT A LIQUID-LIQUID INTERFACE. Journal of Chemical Physics. 1971;54(1):62-&.

[125] Miller DL, Thomas RM. ULTRASOUND CONTRAST AGENTS NUCLEATE INERTIAL CAVITATION IN-VITRO. Ultrasound in Medicine and Biology. 1995;21(8):1059-65.

[126] Ophir J, Parker KJ. Contrast agents in diagnostic ultrasound. Ultrasound Med Biol. 1989;15(4):319-33.

[127] de Jong N, Ten Cate FJ, Lancee CT, Roelandt JR, Bom N. Principles and recent developments in ultrasound contrast agents. Ultrasonics. 1991;29(4):324-30.

[128] Church CC. THE EFFECTS OF AN ELASTIC SOLID-SURFACE LAYER ON THE RADIAL PULSATIONS OF GAS-BUBBLES. Journal of the Acoustical Society of America. 1995 Mar;97(3):1510-21.

[129] Allen JS, May DJ, Ferrara KW. Dynamics of therapeutic ultrasound contrast agents. Ultrasound in Medicine and Biology. 2002 Jun;28(6):805-16.

[130] Stride E, Saffari N. Theoretical and experimental investigation of the behaviour of ultrasound contrast agent particles in whole blood. Ultrasound in Medicine and Biology. 2004 Nov;30(11):1495-509.

[131] Poliachik SL, Chandler WL, Mourad PD, Bailey MR, Bloch S, Cleveland RO, et al. Effect of high-intensity focused ultrasound on whole blood with and without microbubble contrast agent. Ultrasound in Medicine and Biology. 1999 Jul;25(6):991-8.

[132] Coussios CC, Holland CK, Jakubowska L, Huang SL, MacDonald RC, Nagaraj A, et al. In vitro characterization of liposomes and Optison (R) by acoustic scattering at 3.5 MHz. Ultrasound in Medicine and Biology. 2004 Feb;30(2):181-90.

[133] Miller DL, Williams AR. NUCLEATION AND EVOLUTION OF ULTRASONIC CAVITATION IN A ROTATING EXPOSURE CHAMBER. Journal of Ultrasound in Medicine. 1992 Aug;11(8):407-12.

[134] Farny CH, Wu TM, Holt RG, Murray TW, Roy RA. Nucleating cavitation from laser-illuminated nano-particles. Acoustics Research Letters Online-Arlo. 2005 Jul;6(3):138-43.

[135] Miller DL, Kripfgans OD, Fowlkes JB, Carson PL. Cavitation nucleation agents for nonthermal ultrasound therapy. Journal of the Acoustical Society of America. 2000 Jun;107(6):3480-6.

[136] Xu Z, Fowlkes JB, Cain CA. A new strategy to enhance cavitational tissue erosion using a high-intensity, initiating sequence. Ieee Transactions on Ultrasonics Ferroelectrics and Frequency Control. 2006 Aug;53(8):1412-24.

[137] Holt RG, Roy RA, Edson PE, Yang XM. Bubbles and HIFU: the good, the bad and the

ugly. In: Andrew MA, Crum LA, Vaezy S, editors. International Symposium of Therapeutic Ultrasound; 2003; Seattle: Amerian Institute of Physics; 2003. p. 12-131.

[138] Hilgenfeldt S, Lohse D, Zomack M. Sound scattering and localized heat deposition of pulse-driven microbubbles. Journal of the Acoustical Society of America. 2000 Jun;107(6):3530-9.

[139] Edson PL. The role of acoustic cavitation in enahnced ultrasound-induced heating in a tissue-mimicking phantom. Boston: Boston University; 2001.

[140] Yang XM, Roy RA, Holt RG. Bubble dynamics and size distributions during focused ultrasound insonation. Journal of the Acoustical Society of America. 2004 Dec;116(6):3423-31.

[141] Eller A, Flynn HG. Rectified Diffusion during Nonlinear Pulsations of Cavitation Bubbles. The Journal of the Acoustical Society of America. 1963;35:1906.

[142] Eller AI. Growth of Bubbles by Rectified Diffusion. The Journal of the Acoustical Society of America. 1969;46:1246.

[143] Crum LA, Hansen GM. GROWTH OF AIR BUBBLES IN TISSUE BY RECTIFIED DIFFUSION. Physics in Medicine and Biology. 1982;27(3):413-7.

[144] Yang XM. Investigation of bubble dynamics and heating during focused ultrasound insonation in tissue-mimicking materials. Boston: Boston University 2003.

[145] Miller DL, Thomas RM. THRESHOLDS FOR HEMORRHAGES IN MOUSE SKIN AND INTESTINE INDUCED BY LITHOTRIPTER SHOCK-WAVES. Ultrasound in Medicine and Biology. 1995;21(2):249-57.

[146] Miller DL, Creim JA, Gies RA. Heating vs. cavitation in the induction of mouse hindlimb paralysis by ultrasound. Ultrasound in Medicine and Biology. 1999 Sep;25(7):1145-50.

[147] Sokka SD, King R, Hynynen K. MRI-guided gas bubble enhanced ultrasound heating in in vivo rabbit thigh. Physics in Medicine and Biology. 2003 Jan;48(2):223-41.

[148] Sokka SD, Vykhodtseva N, Hynynen K. Cavitation-enhanced ultrasound heating in vivo: Therapy protocols, mechanisms, and acoustic and MRI monitoring. The Journal of the Acoustical Society of America. 2006;119:3227.

[149] Huang J, Holt RG, Cleveland RO, Roy RA. Experimental validation of a tractable numerical model for focused ultrasound heating in flow-through tissue phantoms. Journal of the Acoustical Society of America. 2004 Oct;116(4):2451-8.

[150] Lafon C, Zderic V, Noble ML, Yuen JC, Kaczkowski PJ, Sapozhnikov OA, et al. Gel phantom for use in high-intensity focused ultrasound dosimetry. Ultrasound in Medicine and Biology. 2005 Oct;31(10):1383-9.

[151] Jiang P, Everbach EC, Apfel RE. APPLICATIONS OF MIXTURE LAWS FOR PREDICTING THE COMPOSITIONS OF TISSUE PHANTOMS. Ultrasound in Medicine and Biology. 1991;17(8):829-38.

[152] ANSI technical report: bubble detection and cavitation monitoring. Mellive, NY: Standards Secretariat, Acoustical Society of America; 2002.

[153] Leighton TG. A strategy for the development and standardisation of measurement methods for high power/cavitating ultrasonic fields: review of cavitation monitoring techniques: University of Southampton - Institute of Sound and Vibration Research; 1997.

[154] Pennes HH. Analysis of Tissue and Arterial Blood Temperatures in the Resting Human

Forearm. Journal of Applied Physiology. 1948;1(2):93-122.

[155] Hynynen K. DEMONSTRATION OF ENHANCED TEMPERATURE ELEVATION DUE TO NONLINEAR PROPAGATION OF FOCUSED ULTRASOUND IN DOGS THIGH INVIVO. Ultrasound in Medicine and Biology. 1987 Feb;13(2):85-91.

[156] Clarke RL, Bush NL, ter Haar GR. The changes in acoustic attenuation due to in vitro heating. Ultrasound in Medicine and Biology. 2003 Jan;29(1):127-35.

[157] Zderic V, Keshavarzi A, Andrew MA, Vaezy S, Martin RW. Attenuation of porcine tissues in vivo after high-intensity ultrasound treatment. Ultrasound in Medicine and Biology. 2004 Jan;30(1):61-6.

[158] Hao Y, Prosperetti A. The dynamics of vapor bubbles in acoustic pressure fields. Physics of Fluids. 1999 Aug;11(8):2008-19.

[159] Prosperetti A, Hao Y. Vapor bubbles in flow and acoustic fields. *Microgravity Transport Processes in Fluid, Thermal, Biological, and Materials Sciences*. New York: New York Acad Sciences 2002:328-47.

[160] Konofagou EE, Thierman J, Karjalainen T, Hynynen K. The temperature dependence of ultrasound-stimulated acoustic emission. Ultrasound in Medicine and Biology. 2002 Mar;28(3):331-8.

[161] Vaezy S, Shi XG, Martin RW, Chi E, Nelson PI, Bailey MR, et al. Real-time visualization of high-intensity focused ultrasound treatment using ultrasound imaging. Ultrasound in Medicine and Biology. 2001 Jan;27(1):33-42.

[162] Chan AH, Fujimoto VY, Moore DE, Martin RW, Vaezy S. An image-guided high intensity focused ultrasound device for uterine fibroids treatment. Medical Physics. 2002 Nov;29(11):2611-20.

[163] Seo J, Tran BC, Hall TL, Fowlkes JB, Abrams GD, O'Donnell M, et al. Evaluation of ultrasound tissue damage based on changes in image echogenicity in canine kidney. Ieee Transactions on Ultrasonics Ferroelectrics and Frequency Control. 2005 Jul;52(7):1111-20.

[164] Held RT, Zderic V, Nguyen TN, Vaezy S. Annular phased-array high-intensity focused ultrasound device for image-guided therapy of uterine fibroids. Ieee Transactions on Ultrasonics Ferroelectrics and Frequency Control. 2006 Feb;53(2):335-48.

[165] Coussios CC, Farny CH, Thomas CR, Cleveland RO, Holt RG, Roy RA. Cavitation detection during and following HIFU exposure in vitro. The Journal of the Acoustical Society of America. 2004;115:2448.

[166] Rabkin BA, Zderic V, Crum LA, Vaezy S. Biological and physical mechanisms of HIFU-induced hyperecho in ultrasound images. Ultrasound in Medicine & Biology. 2006;32(11):1721-9.

[167] Thomas CR, Farny CH, Coussios CC, Roy RA, Holt RG. Dynamics and control of cavitation during high-intensity focused ultrasound application. Acoustics Research Letters Online-Arlo. 2005 Jul;6(3):182-7.

[168] Chapelon JY, Dupenloup F, Cohen H, Lenz P. Reduction of cavitation using pseudorandom signals [therapeutic US]. Ultrasonics, Ferroelectrics and Frequency Control, IEEE Transactions on. 1996;43(4):623-5.

[169] Xu Z, Ludomirsky A, Eun LY, Hall TL, Tran BC, Fowlkes JB, et al. Controlled ultrasound tissue erosion. Ieee Transactions on Ultrasonics Ferroelectrics and Frequency Control. 2004 Jun;51(6):726-36.

[170] Sokka SD, Gauthier TP, Hynynen K. Theoretical and experimental validation of a dual-frequency excitation method for spatial control of cavitation. Physics in Medicine and Biology. 2005 May;50(9):2167-79.

[171] Xu Z, Fowlkes JB, Rothman ED, Levin AM, Cain CA. Controlled ultrasound tissue erosion: The role of dynamic interaction between insonation and microbubble activity. Journal of the Acoustical Society of America. 2005 Jan;117(1):424-35.

[172] Lo AH, Kripfgans OD, Carson PL, Fowlkes JB. Spatial control of gas bubbles and their effects on acoustic fields. Ultrasound in Medicine and Biology. 2006 Jan;32(1):95-106.

[173] Roberts WW, Hall TL, Ives K, Wolf JS, Fowlkes JB, Cain CA. Pulsed cavitational ultrasound: A noninvasive technology for controlled tissue ablation (histotripsy) in the rabbit kidney. Journal of Urology. 2006 Feb;175(2):734-8.

FIGURE 1

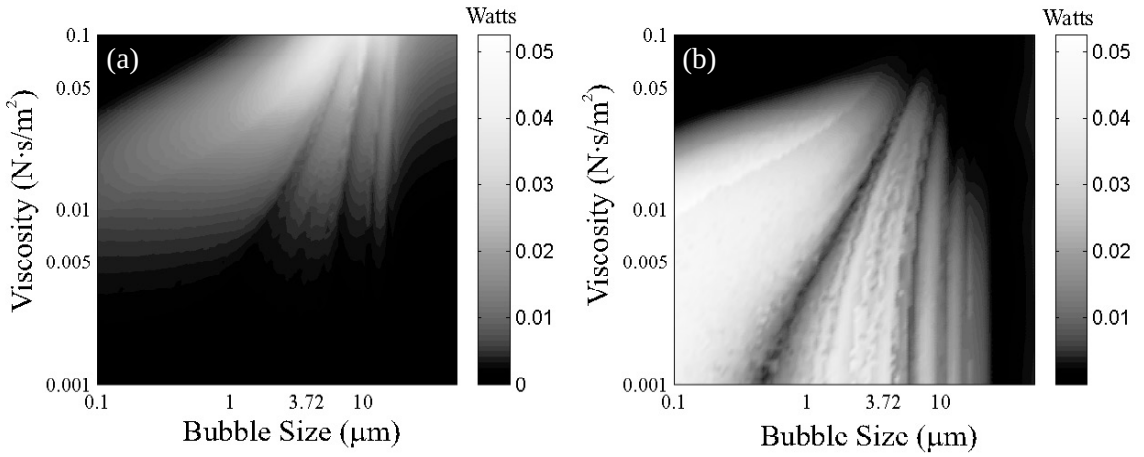

Figure 1: Heating from a single bubble exposed to 1 MHz HIFU at 2.8 MPa pressure amplitude. Power deposited via (a) viscous boundary layer heating and (b) absorption of secondary acoustic emissions (*SAE*) are plotted as a function of the equilibrium bubble radius and the viscosity of the medium [99, 139]. The linear resonance radius at 1 MHz is 3.72 μm.

FIGURE 2

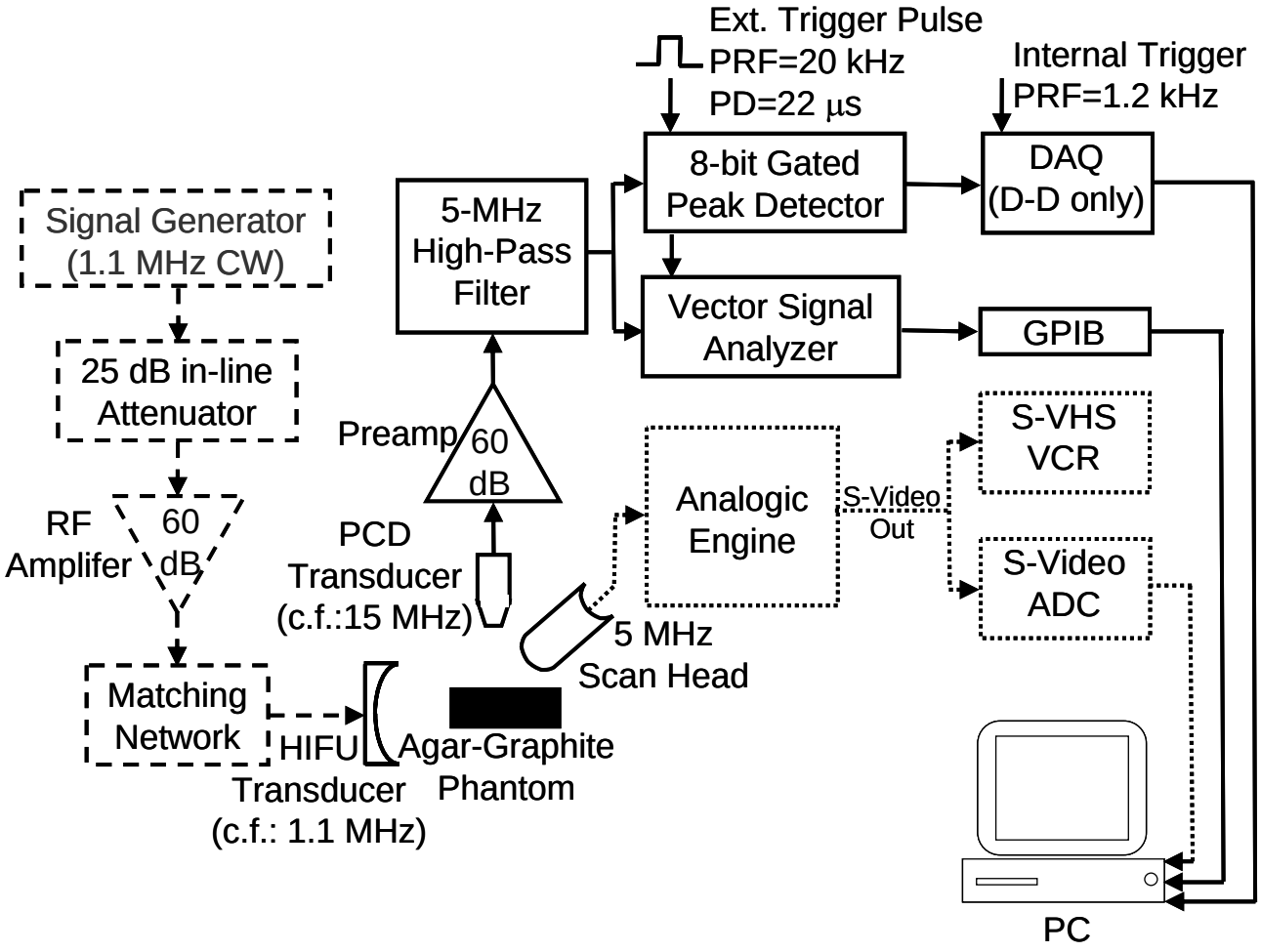

Figure 2: Schematic of the HIFU generation (dashed line), Passive Cavitation Detection (continuous line) and B-mode imaging (dotted line) apparatus.

FIGURE 3

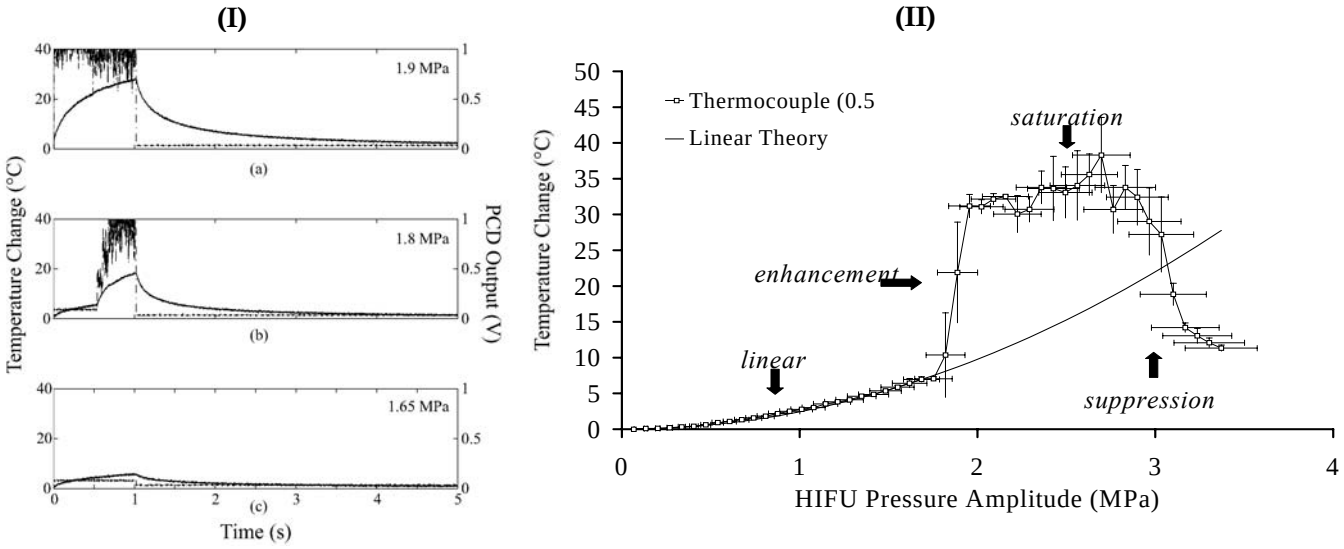

Figure 3 :(I) Measured temperature rise (solid line) and PCD output (dash-dot line) as a function of time for a 1-second 1.1-MHz HIFU insonation of an agar-graphite tissue phantom at three different pressure amplitudes. No inertial cavitation occurs in (c), whilst cavitation onsets halfway through the exposure in (b) and at the start of exposure in (a). In (b) and (c), there is a dramatic increase in the observed rate of heating that is coincident with the onset of inertial cavitation activity. **(II)** Peak temperature rise with respect to ambient conditions versus peak-positive acoustic pressure for the agar/graphite phantom subjected to 700 ms bursts of HIFU. The thermocouple is positioned in the HIFU focal plane 0.5 mm off axis. The 'Linear Theory' curve is computed from the bioheat transfer equation (BHTE) using the known pressure field characteristics. This phantom was only slightly degassed [81, 99, 137].

FIGURE 4

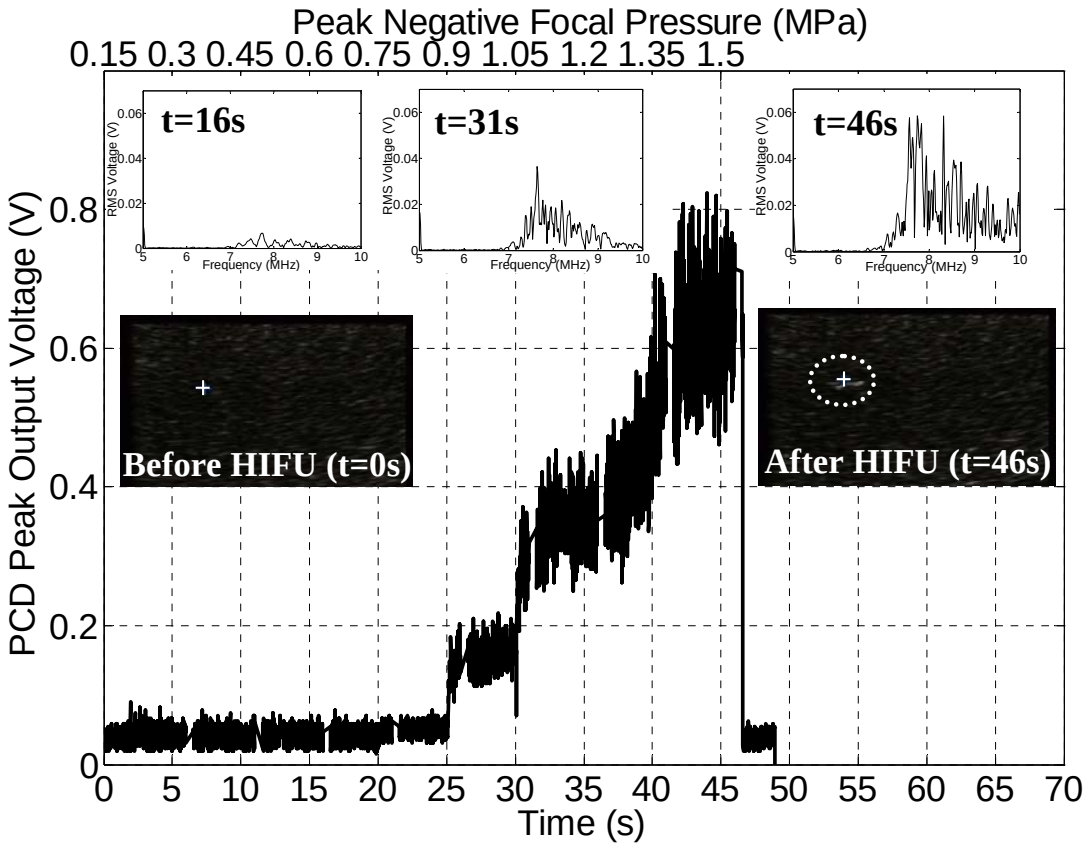

Figure 4: Comparison between Peak PCD output voltage, the frequency spectra of the PCD-received traces and the pre- and post-HIFU B-mode images obtained whilst ramping up the input voltage to the HIFU transducer every 5 seconds (bottom x-axis), thus increasing the peak negative focal pressure in steps of 0.15 MPa (top x-axis). The confocal position of the HIFU, PCD and imaging transducers in the agar-graphite phantom is indicated by the white cross on the B-mode images, with the HFU transducer being to the left of the image, the PCD transducer pointing out of the image and the imaging transducer lying above the image. At a peak negative focal pressure of 0.9 MPa, a sudden increase in peak PCD voltage is observed, which is coincident with a clear jump in broadband noise emissions. However, a hyperechogenic region only becomes visible on the B-mode image at t = 32 s once the HIFU excitation amplitude had been ramped up to 1.35 MPa. This strongly suggests that the appearance of a bright-up on B-mode images cannot be assumed to be coincident with the onset of inertial cavitation activity.

FIGURE 5

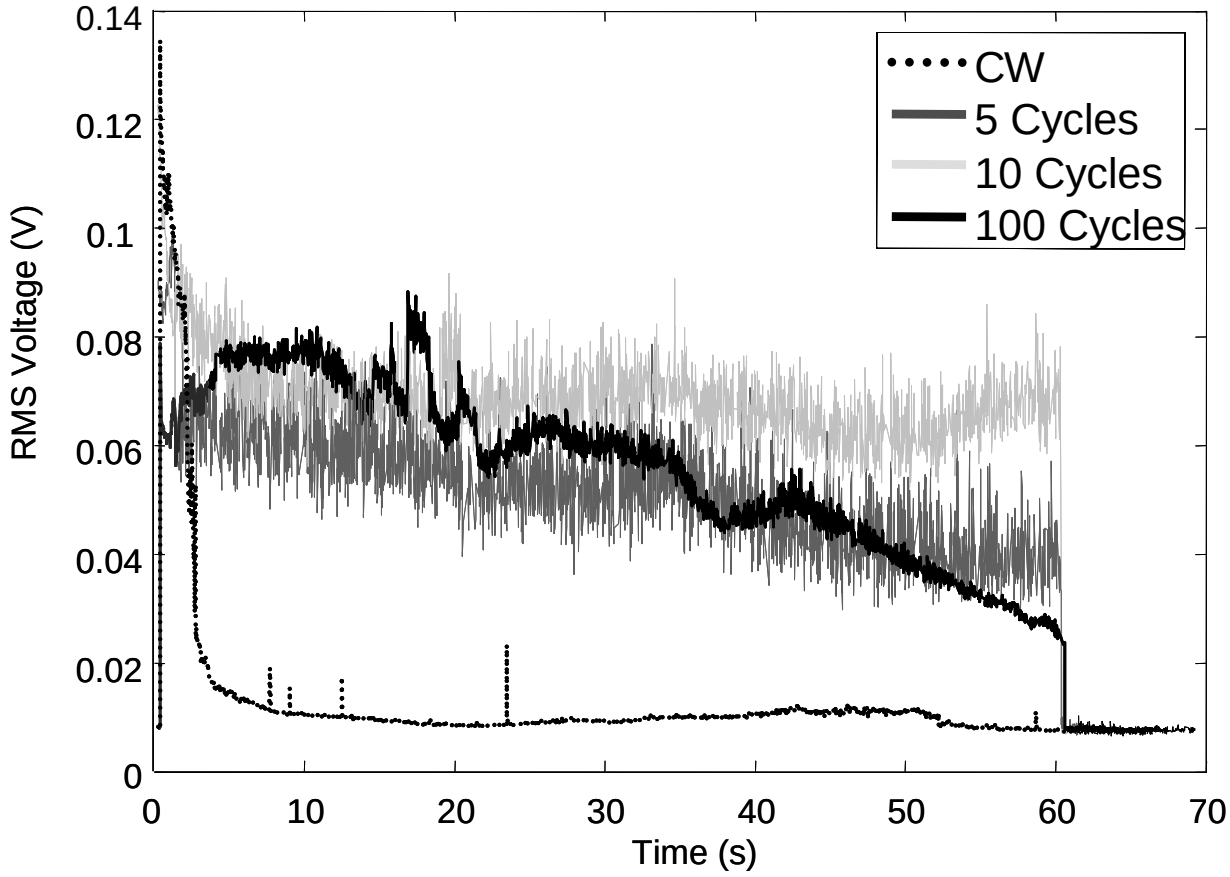

Figure 5: RMS voltage received by a passive cavitation detector (PCD) positioned confocally with the HIFU transducer during excitation of an agar-graphite tissue phantom at a 2.89 MPa peak negative focal pressure amplitude. In all cases, the phantom was exposed to 1-second continuous-wave (CW) excitation, followed by a further 60 seconds of CW exposure (dotted line) or 20% duty-cycle excitation (continuous dark gray, light gray and black lines). A rapid decay in cavitation activity is observed during sustained CW exposure, suggesting movement of the bubble cloud towards the HIFU transducer and out of the field of view of the PCD. Different implementations of 20% duty cycle HIFU excitations, using either 5 cycles (dark grey), 10 cycles (black continuous) or 100 cycles (light grey) on-time, make it possible to sustain cavitation activity in the focal region for extended periods of time. The 10-cycle implementation appears most effective at sustaining the initially generated level of inertial cavitation activity.